IN-46-CR
61477
P-27

# FINAL TECHNICAL REPORT
# ON
# GENERATION OF FIELD-ALIGNED CURRENT IN THE AURORAL ZONE
# (NASA GRANT NAGW-1606)

by

Hideo Okuda

Princeton University, Plasma Physics Laboratory,
Princeton, New Jersey 08543

## ABSTRACT

Generation of a magnetic field-aligned current in the auroral zone connecting the magnetospheric and ionospheric plasmas has been studied by means of a three dimensional particle simulation model. The model is of a magnetostatic variety appropriate for a low beta plasma in which the high frequency transverse displacement current has been eliminated. The simulation model is highly elongated along the magnetic field lines in order to model a highly elongated flux tube in the auroral zone. An enhanced field-aligned current was generated by injection of a magnetospheric plasma across the auroral zone magnetic field at the center of the model. Such a plasma injection may correspond to a plasmoid injection at the geomagnetic tail associated with magnetic reconnection during a substorm or a transverse plasma flow along the low latitude magnetopause boundary layer. The results of the simulations show that the field-aligned current can be enhanced over the thermal current by a factor of 5 - 10 via such injection. Associated with the enhanced current are the electrostatic ion cyclotron waves and shear Alfven waves excited in the auroral zone.

## 1. Introduction

Physics of a plasma in the auroral zone is one of the most interesting and challenging branches of space plasma physics. To note but a few, they include large amplitude electrostatic ion cyclotron waves associated with upward flowing ion beam above 6000 km (Kintner et at., 1979), strong field-aligned currents of 1 - 5 μA/m (Potemra, 1983), generation of accelerated auroral electrons at low altitude (Arnoldy, 1981), acceleration of upward flowing ions perpendicular to the magnetic field leading to formation of ion conics (Gorney et al., 1981) and gereration of field-aligned electric field (Mozer, 1981).

A great deal of observational, theoretical and numerical work has been performed on each of these subjects and these subjects are indeed well understood. There are some attempts to study the interactions and relationships amongst these different physical processes in the auroral zone in order to develop a global macroscopic model taking the microscopic plasma processes into account. Quantitative understanding of cause and effect relationship between the field-aligned current and double layer, for example, is one of such subjects which remains to be resolved from the microscopic point of view. Once these relationships or causalities among various parts of the auroral processes are understood, one can begin to develop a quantitative unified view of auroral plasma physics from the microscopic point of view (Akasofu, 1981). Toward this goal, we developed a three dimensional particle simulation model in which generation of a field-aligned current in the auroral zone and its effect on the various microscopic processes can be studied in a self-consistent manner. The model is described in Section 2 in which a three dimensional elongated grid was used in order to model a highly elongated flux tube in the auroral zone. In Sec. 3, results of the simulations are presented for the cases with and without a plasma injection demonstrating that a field-aligned current can be enhanced over the thermal level when a plasma is injected into the auroral zone. Concluding remarks are given in Sec. 4.

## 2. Simulation Model

Here we briefly describe the simulation model developed for the present study. In order to study generation of field-aligned currents and microscopic plasma processes associated with the current, we assume in

our model that the driving mechanism for the current is the perpendicular injection of a magnetospheric plasma into the auroral zone ionosphere. Such an injection may take place during a substorm at the geomagnetic tail region or at the low latitude boundary layer at the flanks of the magnetopause. The model is sketched in Fig.1 where the three dimensional cylinder elongated along the magnetic field corresponds to the auroral zone. The model can be considered part of the flux tube in the auroral zone connecting the magnetosphere and the ionosphere. In that case one may use a periodic boundary condition in three directions. On the other hand, the model can be considered to represent an entire flux tube between the two polar regions of the ionosphere located at the both ends of the model while the magnetospheric plasma is located at the middle of the model. In that case proper boundary condition for the potential ø is $ø(z=0)=ø(z=Lz)=0$.

In order to model a highly elongated flux tube of a plasma, the spatial grid used in the simulations is highly elongated using cubic splines which is known to suppress numerical instabilities (Okuda et el., 1979). In this model the grid size in the z-direction along the magnetic field can be 10 - 100 times that of the grid size in the perpendicular x-y plane. This is very important in modeling the auroral zone since the flux tube in this region can be a few thousand km long while its transverse dimension is a few tens or hundred km wide.

In order to test the validity of the model developed, test runs were made. Figures 2 and 3 show results of such simulation for a plasma near thermal equilibrium in which the plasma density is spatially uniform and the velocity distribution is a Maxwellian. Such a run is important in order to confirm the validity of the code by comparing the fluctuations from the simulation with theoretical predictions available for a plasma in thermodynamic equilibrium. Shown in Figs. 2 and 3 are the electrostatic and magnetic fluctuations obtained from the simulation by time-averaging the measured electric and magnetic fields. Both the electric and magnetic field energies per Fourier mode (k-space) agree well with the theoretical predictions given by

$$V\frac{|E_k|^2}{4\pi T_e} = \frac{1}{1+k^2\lambda_D^2 S^{-2}} \tag{1}$$

$$V\frac{|B_k|^2}{4\pi T_e} = \frac{1}{1+k^2c^2S^{-2}/\omega_{pe}^2} \tag{2}$$

where

$$S^2 = \exp(-k^2a^2)\,\frac{\sin^4 k_x\Delta x/2\,\sin^4 k_y\Delta y/2\,\sin^8 k_z\Delta z/2}{(k_x\Delta x/2)^4\,(k_y\Delta y/2)^4\,(k_z\Delta z/2)^8} \tag{3}$$

is the effective shape factor used in the simulations. Linear interpolation was used in the transverse x-y plane while cubic interpolation was carried out in the z-direction where the grid is highly elongated. Such high order interpolation was required for the numerical stability in that directio (Okuda et al.,1979). Note that we used gaussian shaped finite-size particles with its width "a".

In order to model generation of field-aligned current in the auroral zone, a plasma is injected perpendicular to the magnetic field. Such an injection can be considered a plasmoid injection at the geomagnetic tail via magnetic reconnection or a plasma penetration across the magnetopause flank at the low latitude boundary layer. Owing to the difference between the perpendicular motions of the ions and the electrons, a charge separation will be set up across magnetic field generating perpendicular electric field. Such an electric field is then short-circuted by the field-aligned current mostly carried by the ionospheric electrons in the auroral zone. When the transverse velocity caused by the perpendicular electric field is large enough overcoming viscosity damping, Kelvin-Helmholtz instability can develop generating large scale vortices across magnetic field (Okuda and Hiroe, 1987).

Shown in Figs. 4 and 5 are results from such simulations carried out in a 2-1/2 dimensional electrostatic code in an external magnetic field given by $\underline{B}$ = (Bx,0,Bz) with Bz >> Bx. A plasmoid is injected at the middle of the y coordinate in the x direction across magnetic field. The scatter plots for the ions shown in Fig.4 at four different time steps show that the ripples at the plasma boundary develop into large scale vortices. The corresponding electrostatic potential contours shown in Fig. 5 indicate the generation of large scale structures from smaller contours.

According to the theory of Hasegawa and Sato (1979), vortex motion of a plasma generates a field-aligned current given by

$$J_{\parallel} = B \int \left[\frac{\rho}{B}\frac{d}{dt}\left(\frac{\Omega}{B}\right) + \frac{2}{B^2}\underset{\sim}{J}_{\perp}\cdot\underset{\sim}{\nabla}B - \frac{1}{\rho B}\underset{\sim}{J}_{in}\cdot\underset{\sim}{\nabla}\rho\right]d\ell_{\parallel} \qquad (4)$$

whete $\underline{\Omega}$ is the vorticity, $\underline{J}_{\perp}$ is the plasma current across magnetic field and $\underline{J}in = -(c\ /B\ )(d\underline{v}/dt)x\underline{B}$. Physically speaking, the motion of the ions and electrons across magnetic field generates charge separation because

of the presence of the ion finite-gyroradius and inertia, magnetic field curvature and gradients. Once generated, such charge separation can be neutralized by the motion of the electrons along field lines thereby generating a field-aligned current. Because of the presence of the ionosphere, each field line is not independent so that a macroscopic current and hence potential structures can develop along and across field lines. Depending on the strength of the field-aligned current, various microinstabilities may be excited in the auroral zone as we shall see in the next Section.

## 3. Results of the Simulations

Using the simulation model described, several runs were made in order to study field-aligned current generation by injection of a plasma across magnetic field. First, results of the simulation without plasma injection are shown which are then compared with those with injection. Typical simulation parameters are: system size Lx.Ly.Lz = 128.128.1280 Debye cube (64.64.64 grid points),ion to electron mass ratio = 100, magnetospheric to ionospheric plasma temperature = 9, time step of integration = 5 in the unit of the electron plasma frequency.

Shown in Fig. 6 and 7 are the results of the simulation at t =400 without plasma injection in which the ionospheric plasma was initially distributed uniformly in the three dimensional space. Note the system is highly elongated along the magnetic field, however, it is still only about 1000 Debye length long corresponding to only a few hundred meters or so. We therefore assume that the simulated plasma is only part of much larger plasma in an auroral zone flux tube extending a few thousand km so that a periodic boundary condition was used in three directions. The four frames in Figs. 6 and 7 correspond to four locations along the z direction located at (a) z= Lz/4, (b) z=Lz/2, (c) z=3Lz/4, and (d) z=Lz. Each arrow in Fig. 6 represents a field-aligned current Jz at the location in the two-dimensional x-y plane. Arrows may be pointing upward corresponding to the upward flowing current or downward corresponding to the downward flowing field-aligned current. It is clear that the currents are more or less uniformly distributed in the x-y plane as well as along the magnetic field. The strength of the current will be amplifield as we shall see next when a plasma is injected into the auroral zone. The potential contours shown in Fig. 7 indicate thermal fluctuations of the system whose spatial size and the amplitude become larger with the injection.

We shall now study the effect of a plasma injection into the ionospheric plasma in the auroral zone. A magnetospheric plasma with the density equal to that of the ionosphere but with its temperature 9 time the ionospheric temperature was injected across magnetic field at the center of the system. The density of the injected plasma is localized at the center and is gaussian shaped in three directions with the half-width a quarter of the system size in three directions. The initial injection speed was subsonic and it is one-half of the magnetospheric ion thermal speed pointing to the x-direction. Once the magnetospheric plasma is injected, both the ions and electrons move across and along magnetic field. The motion in the perpendicular x-y plane tends to generate a charge separation since the ions move across magnetic field while the electrons are trapped by the magnetic field. The charge separation thus generated can be neutralized by the ionospheric electrons flowing along the magnetic field thereby generating a field-aligned current.

Shown in Fig. 8 are the scatter plots of the electrons (top) and ions (bottom) injected into the magnetic field at t=200. The left column, (a) and (d), are in the x-y plane, the middle, (b) and (e), in the x-z plane , and the right, (c) and (f) are in the y-z plane respectively. One can observe that in the x-y plane, electrons shown in (a) more or less remain at the center of the system while the ions moved to the left and downward. The ion motion is caused by the initial injection and subsequent gyration in the magnetic field. In the x-z and y-z planes, electrons rapidly spread out along the magnetic field while ions cannot follow the electrons as shown in (b) and (e), and (c) and (f). It is clear from (e) and (f) that the ions moved in the direction of the injection across magnetic field.

Shown in Fig. 9 are the corresponding potential contours in the x-y plane at four different z locations as before at: (a) z=Lz/4, (b) z=Lz/2, (c) z= 3Lz/4, and (d) z=Lz at t=200. Comparing Fig. 9 with Fig.7 without injection, one can find that the size of the contours are generally larger and their amplitude is also larger by a factor 5 or so. While it is true that the amplification was much larger in two dimensional simulations shown in Figs. 4 and 5 where no charge neutralization took place by the field-aligned current, an enhanced current can be generated in three dimensions.

Similar coalescence of the potential contours can take place for the magnetic field structure as shown in Fig. 10 where the z-component of the vector potential Az is shown at four locations along z as before.

At each location in z, the contour is dominated by a few large vortices corresponding to the field-aligned current filament. Both positive and negative contours exist which correspomd to the upward and downward going currents. Coalescence of smaller magnetic islands into larger ones are well-known in magnetohydrodynamics

Let us now look at the field-aligned current whether or not it was indeed enhanced over the thermal current due to plasma injection. Shown in Fig. 11 is the field-aligned current carried by the ionospheric plasmas at the four z locations as before at t=200. comparing these with the current in Fig. 6 for the ionospheric plasma without injection, the magnitude is enhanced typically by a factor 3 or so in the presence of injection. Localized current filaments are found which may be moving upward or downward along field fines depending on the pattern of plasma injection.

Shown in Fig. 12 are the similar field-aligned current carried by the injected magnetospheric plasma. These currents are more or less localized at a location where the plasma density is the maximum as seen in Fig. 8. It is interesting to note that the direction of the current carried by the magnetospheric plasma is pointing only one direction at each two-dimensional x-y plane. In Fig.12 (a), for example, the current is pointing upward everywhere while it is downward in Fig. 12 (c). These field-aligned current must be closed by the perpendicular cross field current in order for the plasma to maintain charge neutrality.

The total current which is the sum of the ionospheric and magnetospheric currents are shown in Fig. 13 in the same format. Again the magnitude of the total current is several times larger than the corresponding current in a plasma without injection. One can observe a presence of localized current filaments in the x-y plane. In Fig. 13 (c), for example, a downward current filament can be seen at the outer edge of the system while in the middle, an upward moving current filament can be seen. The magnitude of the total current can exceed locally the ionospheric ion thermal speed and therefore one may expect excitation of various plasma waves by the field-aligned current. Local velocity distributions were measured for both the ionospheric ions and electrons confirming that the field-aligned current is primarily carried by the ionospheric electrons moving along magnetic field whose local drift speed can exceed ion thermal speed.

In order to detect the waves generated by the field-aligned current, power spectrum was calculated for both the electrostatic and vector potentials for several Fourier modes in the presence of plasma injection. Shown in Fig. 14 are the measured power spectrum for the electrostatic potential of the mode (3,6,0), (a), and for the vector potential of the mode (0,6,6), (b). One can identify the frequency of the electrostatic potential is close to the ion gyrofrequency, while the magnetic fluctuations correspond to the shear Alfven waves. The amplitude of these waves are an order of magnitude larger than the corresponding thermal plasma without injection. It is clear that the excitation of these waves above the thermal level must by caused by the field-aligned curret (Kindel and Kennel, 1971).

## 4. Concluding Remarks

We have developed a three dimensional magnetostatic particle simulation model in a low beta plasma in order to study generation of field-aligned current and the related phenomena in the auroral zone. The model is a low beta magnetostatic code with the highly elongated spatial grid along the magnetic field in order to study the auroral zone plasma in a highly elongated flux tube. The validity of the code was demonstrated by simulating a plasma near thermodynamic equilibrium. The results of the simulations were in good agreement with plasma theory. The code was then used to study an enhaced field-aligned current generated by injection of a magnetospheric plasma across magnetic field. Such a plasma injection may take place at the geomagnetic tail associated with magnetic reconnection during substorm or plasma flow at the magnetopause in the low latitude magnetopause boundary layer.

The results of the simulations with injection confirmed generation of enhanced field-aligned current associated with injection over the corresponding thermal plasma. The enhanced current is primarily carried by the ionospheric electrons whose speed can exceed the ion thermal speed. As a consequence, both the electrostatic ion cyclotron and shear Alfven waves are generated in the auroral zone. During the course of this work, a number of talks were gives to report the progress (Hwang and Okuda. 1989; Okuda,1991) and a final full length article is being prepared for submission to the Journal of Geophysical Research (Okuda, 1992).

## ACKNOWLEDGEMENTS

This work was supported by the NASA Grant NAGW -1606 and the Department of Energy Contract DE-AC02-76-CHO3073 to Princeton University. Part of the computing was carried out on the Cray Y-MP at the San Diego Super Computer Center supported by the National Science Foundation.

## REFERENCES

Akasofu, S.-I., Auroral arcs and auroral potential structure, in Physics of auroral arc formation, edited by S.-I. Akasofu and J.R. Kan, American Geophysical Union, Washington, DC, pp. 1-14, 1981.

Arnoldy, R.L., Review of auroral particle precipitation, in Physics of auroral arc formation, edited by S.-I. Akasofu and J.R. Kan, American Geophysical Union, Washington, DC, pp. 56-66, 1981.

Gorney, D.J., A. Clarke, D. Crowley, J. Fennell, J. Luhman, and P. Mizera, The distribution of ion beams and conics below 8000 km, J. Geophys. Res., 86, 83, 1981.

Hasegawa, A., and T. Sato, Generation of field aligned current during substorm, in Dynamics of the Magnetosphere, D. Reidel, pp. 529-542, 1979.

Hwang, Y.S., and H. Okuda, Generation of field-aligned current in the auroral zone, EoS, 70, 1265, 1989.

Kan, J.R., Towards a unified theory of discrete auroras, Space Science Rev. 31, 71, 1981.

Kindel, J.M., and C.F.Kennel, Topside current instabilities, J. Geophys. Res., 76, 3055, 1971.

Kintner, P.M., M.C. Kelley, R.D. Sharp, A.G. Ghielmetti, M. Temerin, C. Cattell, P.F. Mizera, and J.F. Fennell, Simultaneous observations of energetic (keV) upstreaming ions and electrostatic hydrogen cyclotron waves, J. Geophys. Res., 84, 7201, 1979.

Mozer, F.S., The low altitude electric field structure of discrete auroral arcs, in Physics of auroral arc formation, edited by S.-I. Akasofu and J.R. Kan, American Geophysical Union, Washington, DC, pp. 136-142, 1981.

Okuda, H., and S. Hiroe, Diffusion of a plasma in a plasma subject to neutral beam injection, Phys. Fluids 30, 1160, 1987.

Okuda, H., W.W.Lee, and C.Z. Cheng, Electrostatic and magnetostatic particle simulation models in three dimensions, Comp. Phys. Comm. 17, 233, 1979.

Okuda, H., Generation of field-aligned current in the auroral zone, AGU Chapman conference on Auroral Plasma Dynamics, October, 1991, Minneapolis.

Okuda, H., Numerical simulation of the generation of field-aligned current in the auroral zone, to be submitted to J. Geophys. Res., 1992.

Potemra, T.A., Birkeland current: Present understanding and some remaining questions, in High-latitude space plasma physics, edited by B. Hultqvist and T. Hagfors, Plenum, pp. 355-376, 1983.

## FIGURE CAPTIONS

Fig. 1 Sketch of the three dimensional simulation model in the auroral zone. A plasmoid can be injected at the middle of the system, z=0.5Lz. Both periodic and ionospheric boundary conditions can be imposed at z=0 and z=Lz.

Fig. 2 Test of the three dimensional model for a plasma near thermal equilibrium: Electrostatic fluctuation energy as a function of the Fourier mode. The solid curve is the theoretical prediction.

Fig. 3 Test of the three dimensional model for a plasma near thermal equilibrium: Magnetic fluctuation energy as a function of the Fourier mode. The solid curve is the theoretical prediction.

Fig. 4 Results of a 2-1/2 dimensional electrostatic simulation in which a plasma is injected across magnetic field. Scatter plots of the injected ions at (a) t=100, (b) t=200, (c) t=300, (d) t=400 where the time is in the unit of the electron plasma frequency.

Fig. 5 Electrostatic potential contours corresponding to the flow pattern in Fig. 4. Note the formation of large scale positive and negative contours resulting from plasma injection.

Fig. 6 Plots of the field-aligned current in the z-direction, Jz, in the x-y plane at four different locations in the z-direction: (a) z=Lz/4, (b) z=Lz/2, (c) z=3Lz/4, and (d) z=Lz when there is no plasma injection. The field-aligned currents are more or less randomly distributed. The magnitude of the current is modest and its maximum is about a quarter of the thermal current defined by env . The time step in this plot is t=400.

Fig. 7 Plots of the electrostatic potential contours in the x-y plane at four different locations along the z-direction as in Fig. 6 at t=400. Positive and negative potential peaks are randomly distrubuted in all these plots and no coherent large structures are seen.

Fig. 8 Scatter plots of the injected magnetospheric electrons (top) and ions (bottom) in the x-y (a,d), x-z (b,e), and y-z (c,f) plane. Note in the x-y plane, ions can spread out faster than the electrons while in the x-z and y-z planes, electrons spread out rapidly along magnetic field.

Fig. 9 Plots of the two-dimensional electrostatic potential contours in the x-y plane at four different z locations as in Fig. 7. Note the magnitude of the contours are larger than the thermal level.

Fig.10 Plots of the two-dimensional vector potential Az contours in the x-y plane at four different z locations as in Fig. 9.

Fig.11 Plots of the field-aligned current carried by the ionospheric plasma in the presence of plasma injection in the x-y plane at four different z locations as in Fig. 6. Note the magnitude of the current intensity is enhaced over the thermal level.

Fig.12 Plots of the field-aligned current carried by the magnetospheric plasma at four different z locations as in Fig. 11.

Fig. 13 Plots of the total field-aligned current in the x-y plane at four different z locations as in Fig. 12. The amplitude of the total current is several times over the thermal level.

Fig.14 Power spectrum for the (a) (3,6,0) mode for the electrostatic fluctuations and for the (b) (0,6,6) mode for the magnetic fluctuations. The peaks of the spectra correspond to the ion cyclotron frequency and the shear Alfven frequency.

#88T0053

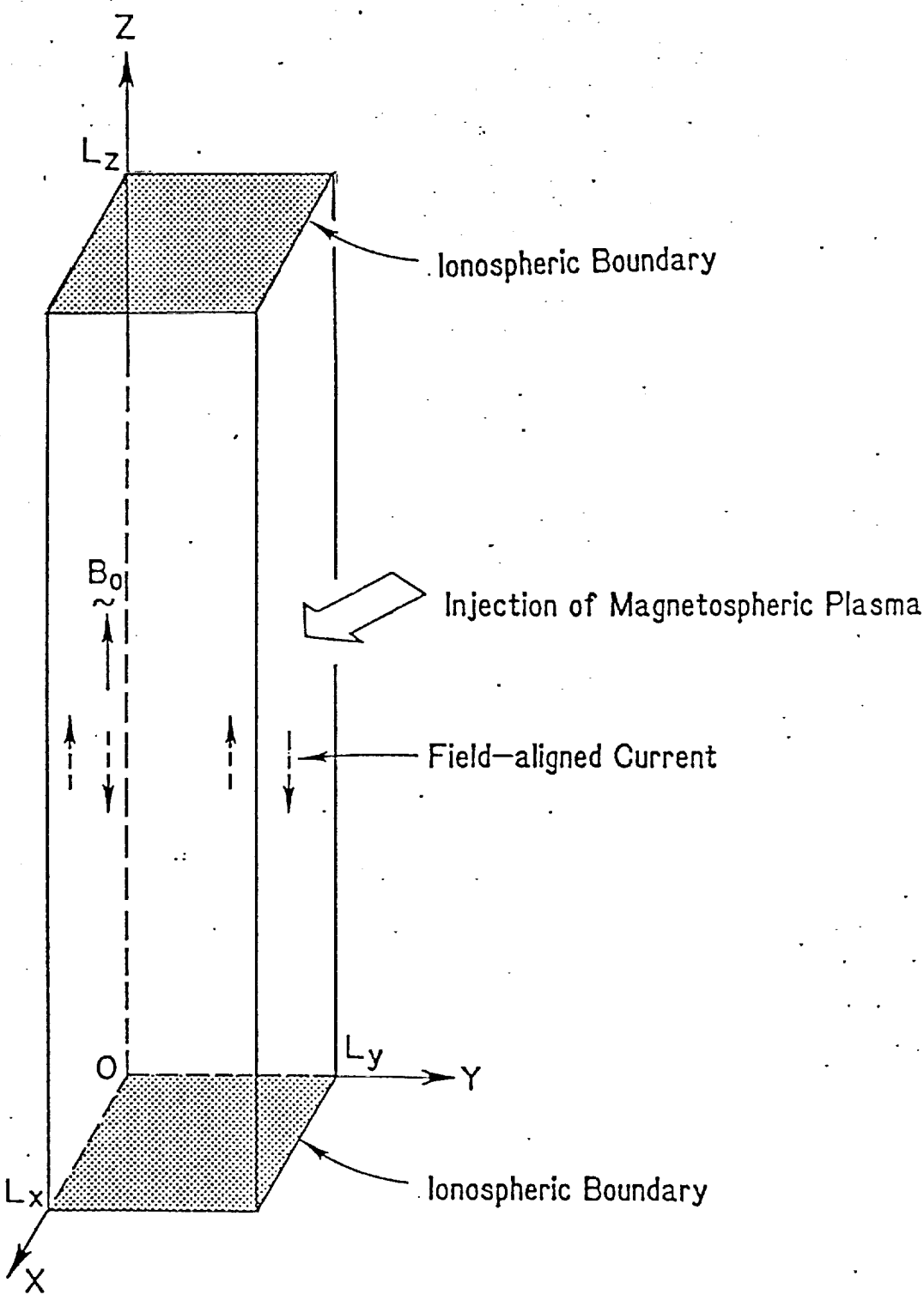


FIG. 1

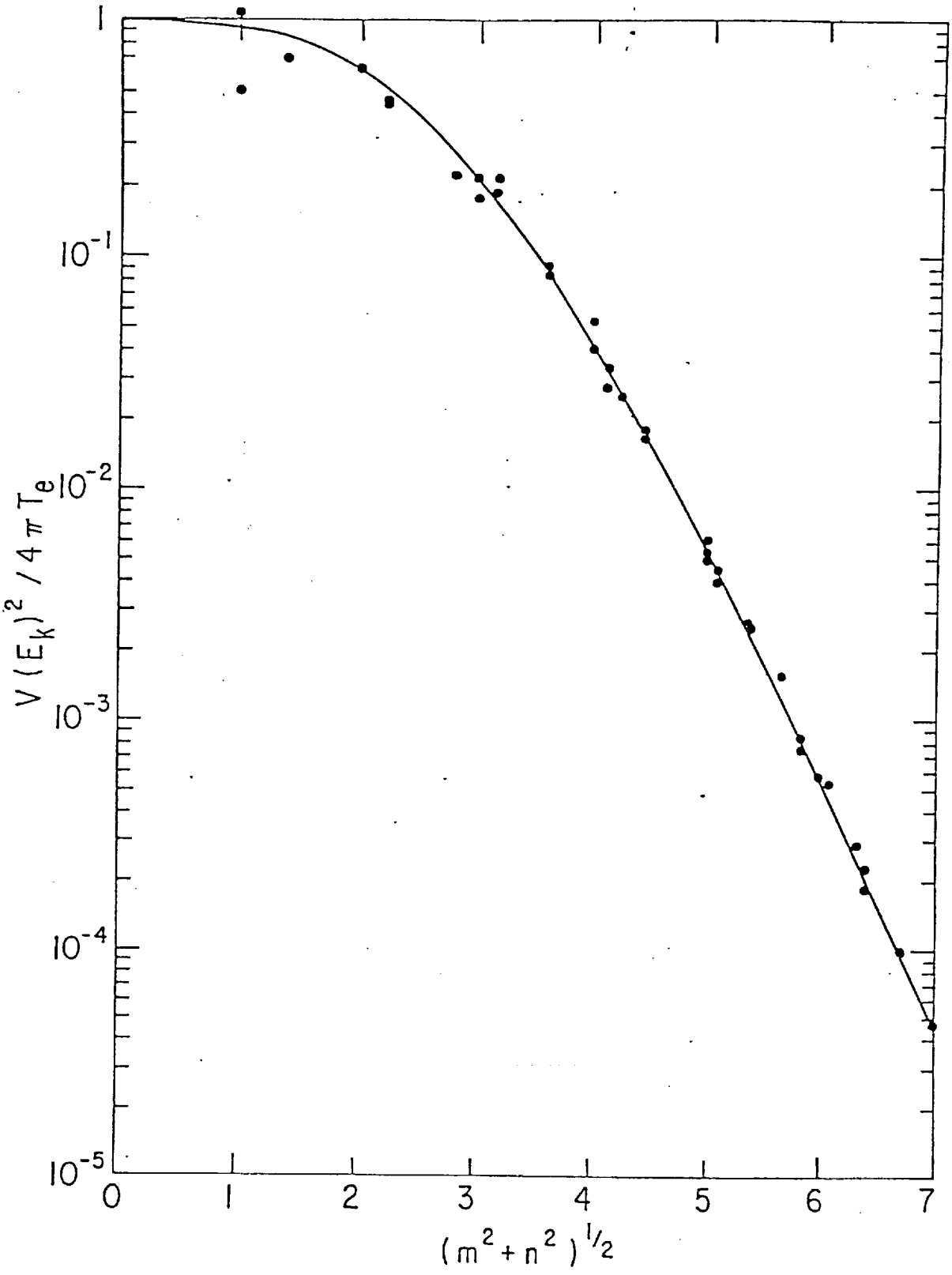


FIG. 2

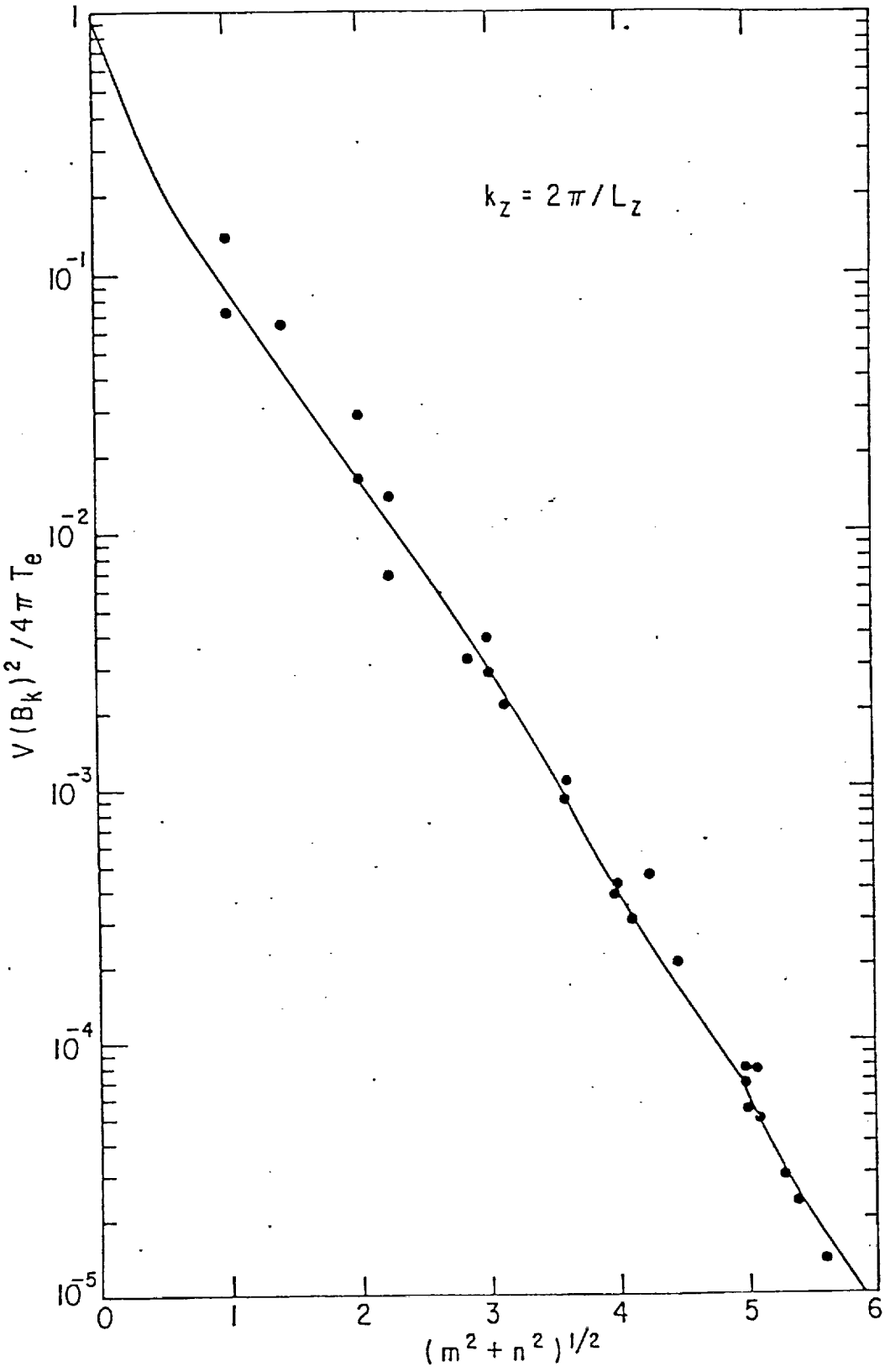


FIG. 3

782168

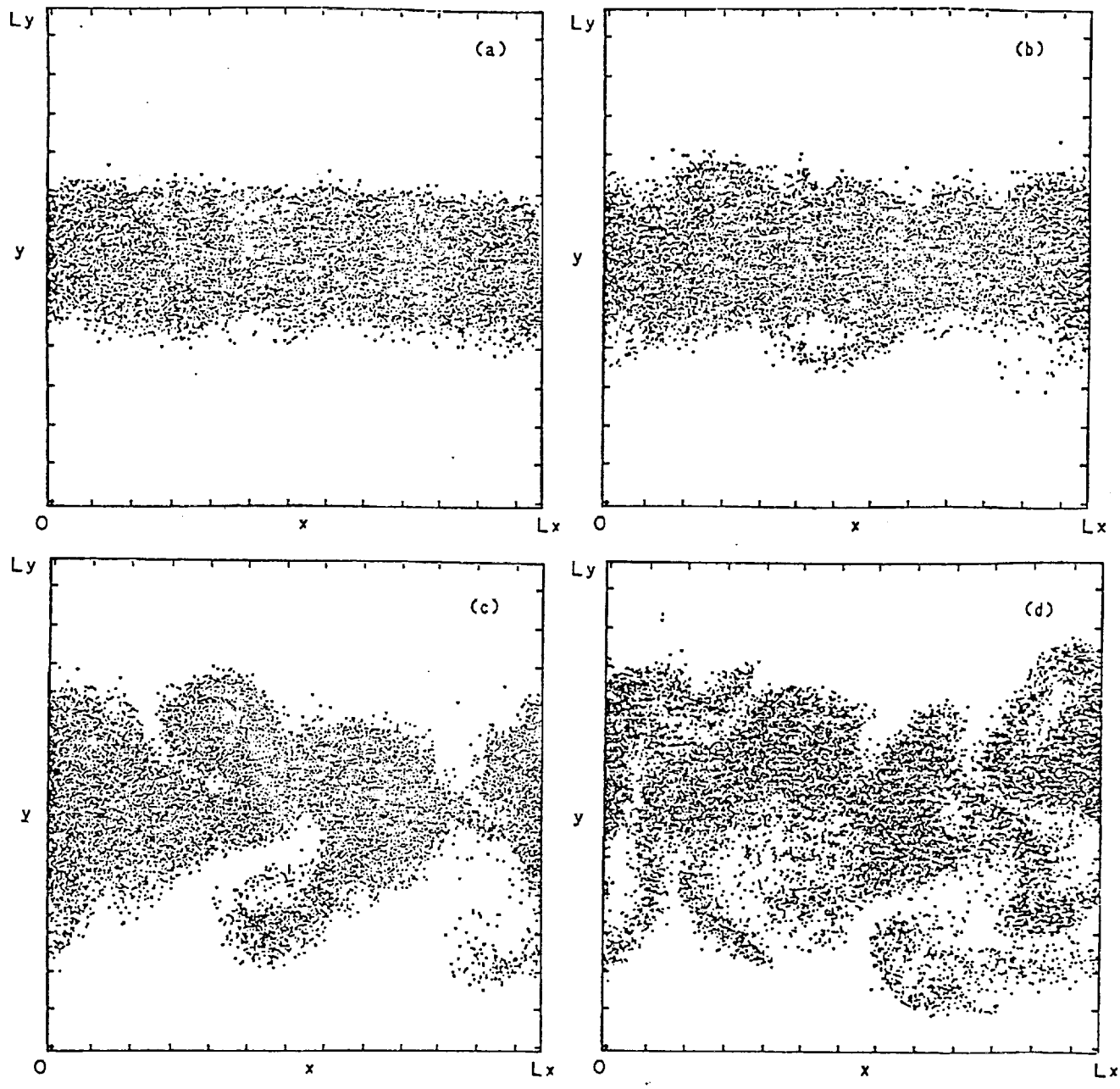


FIG. 4

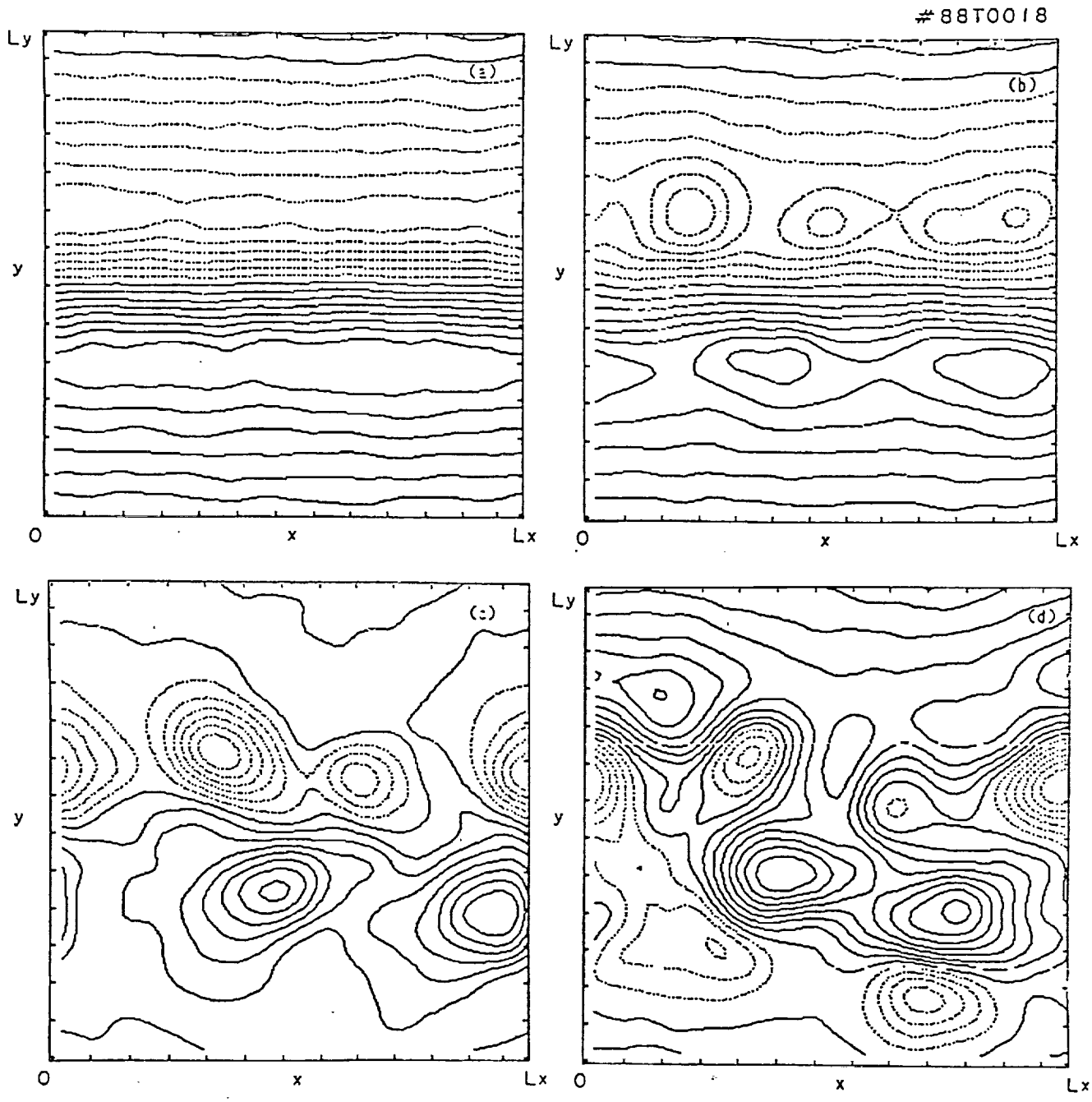


FIG. 5

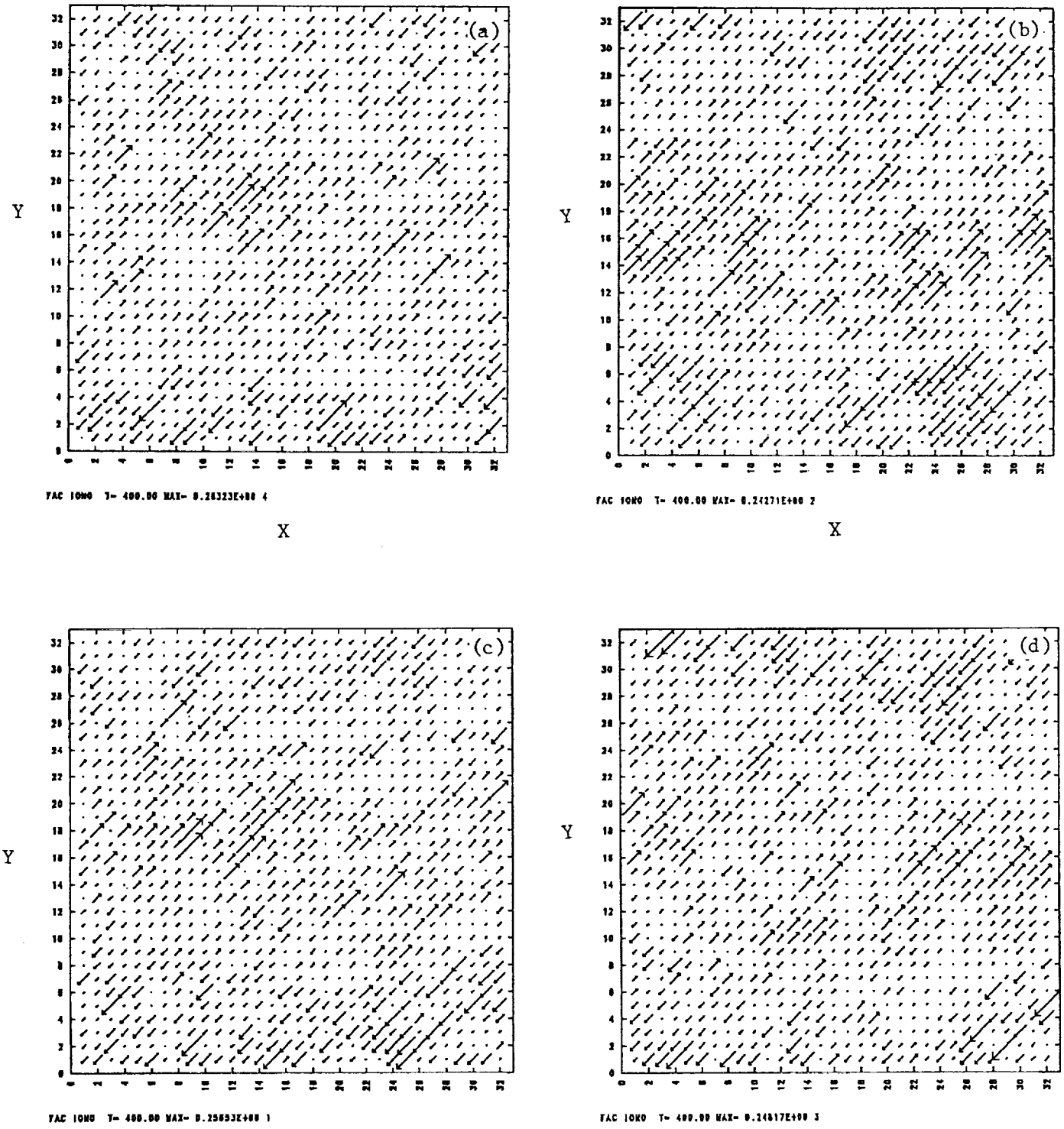


FIG. 6

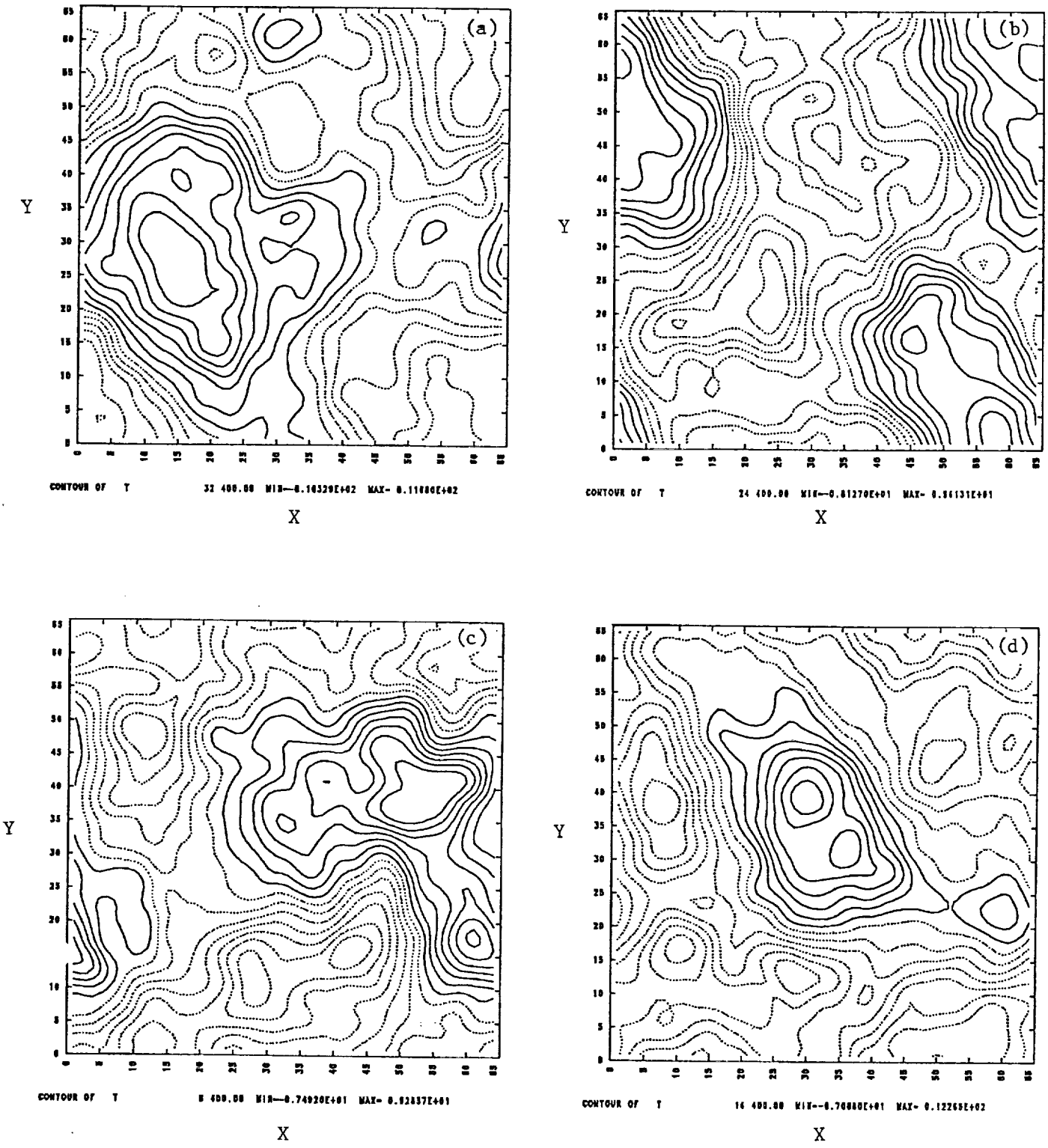


FIG. 7

FIG. 8

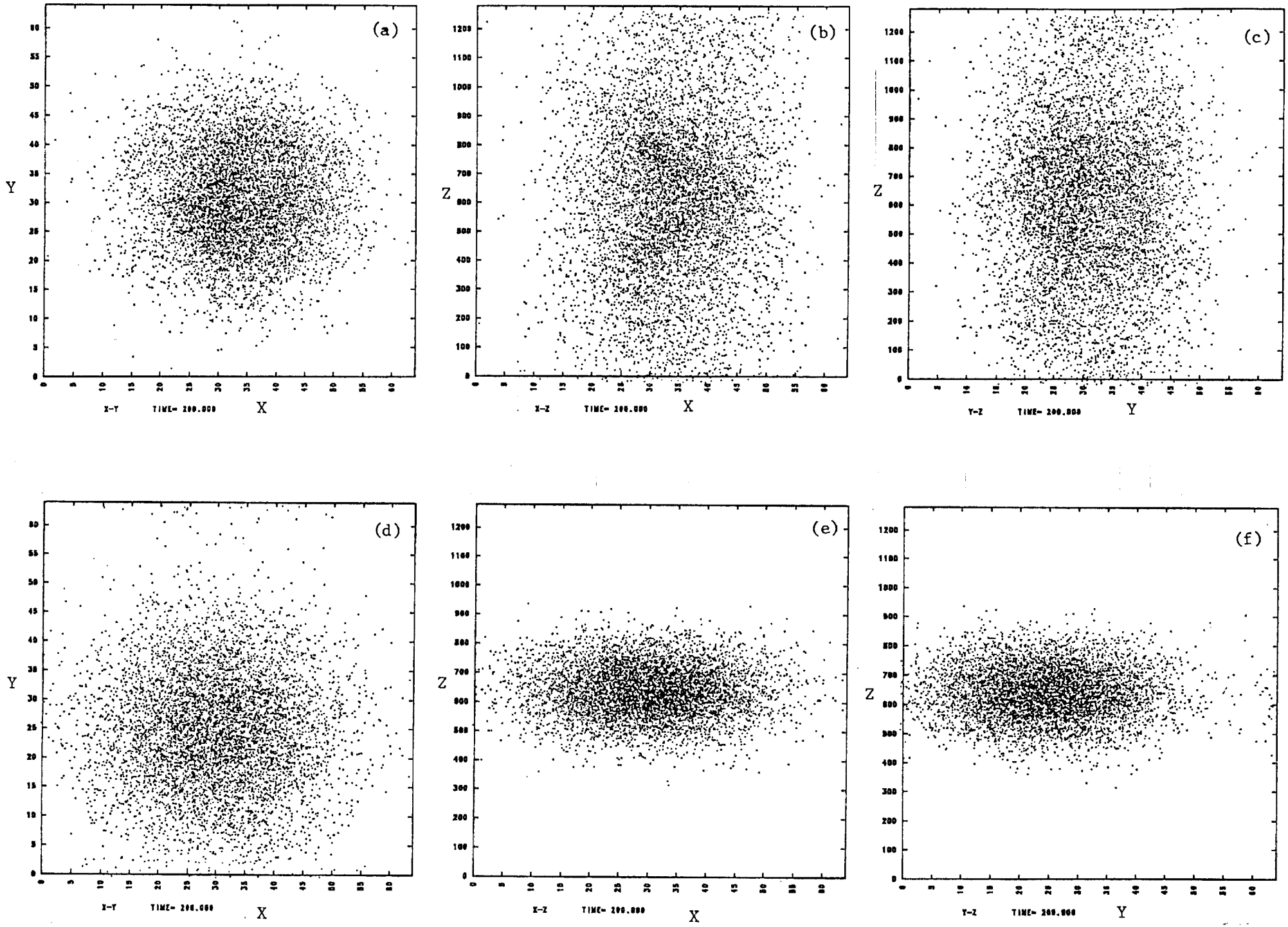

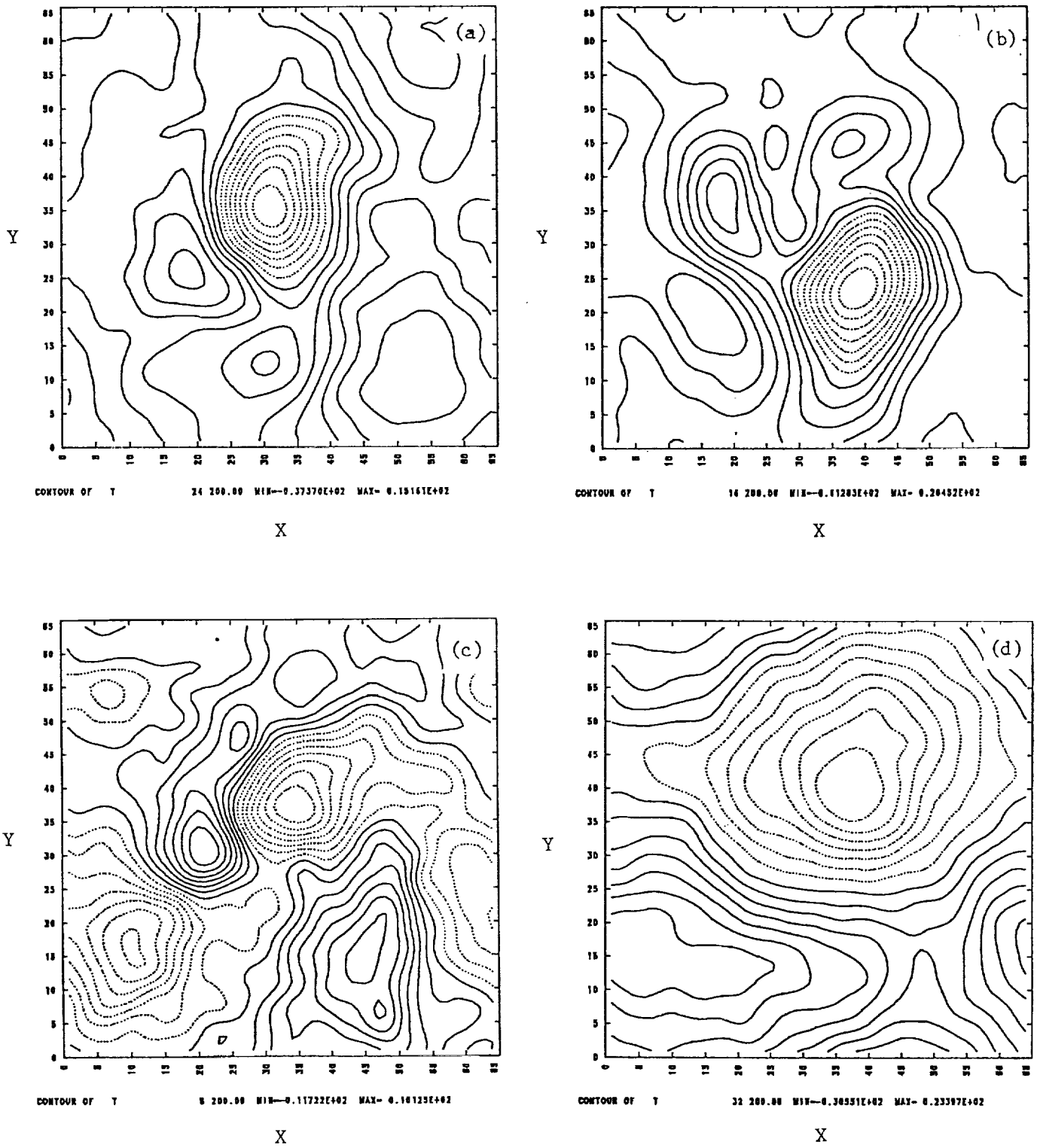


FIG. 9

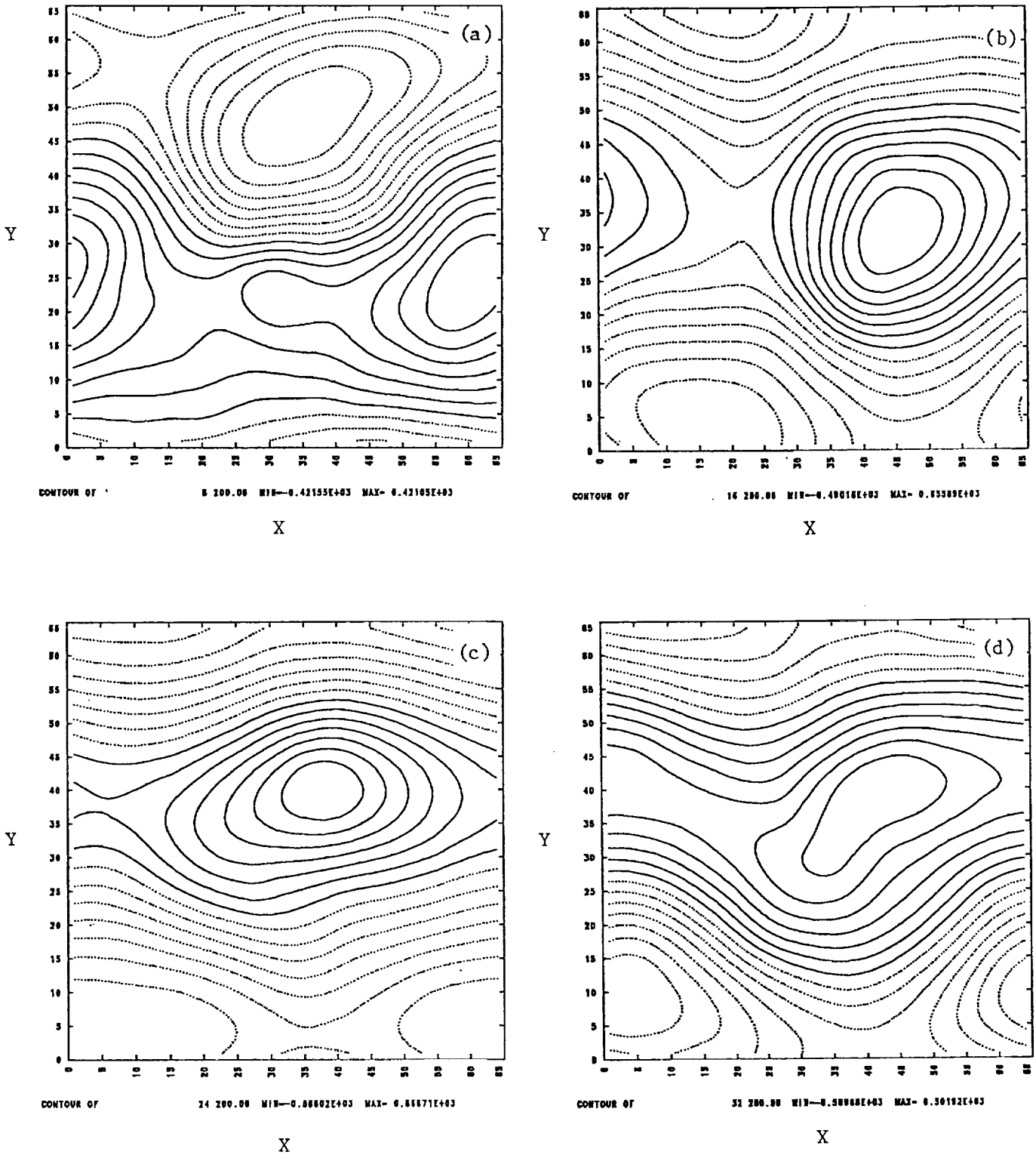


FIG. 10

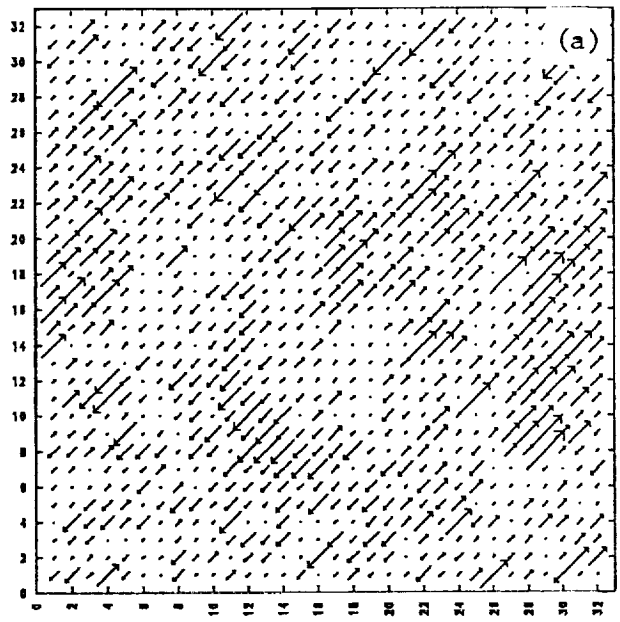


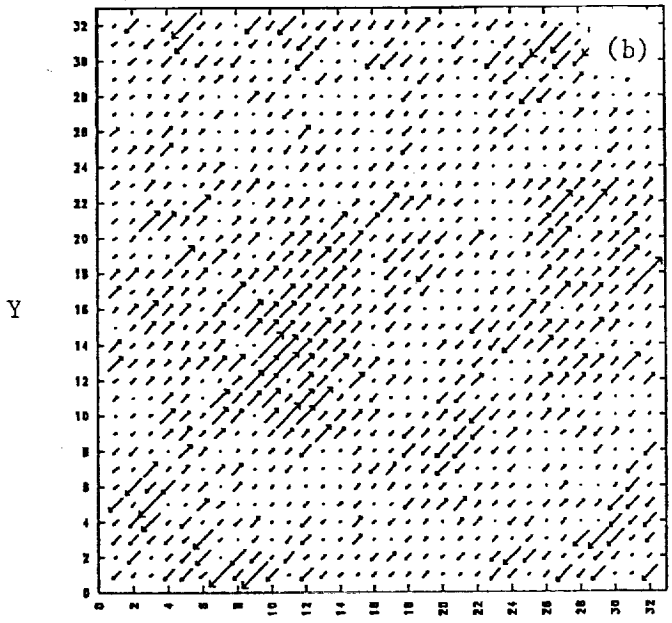


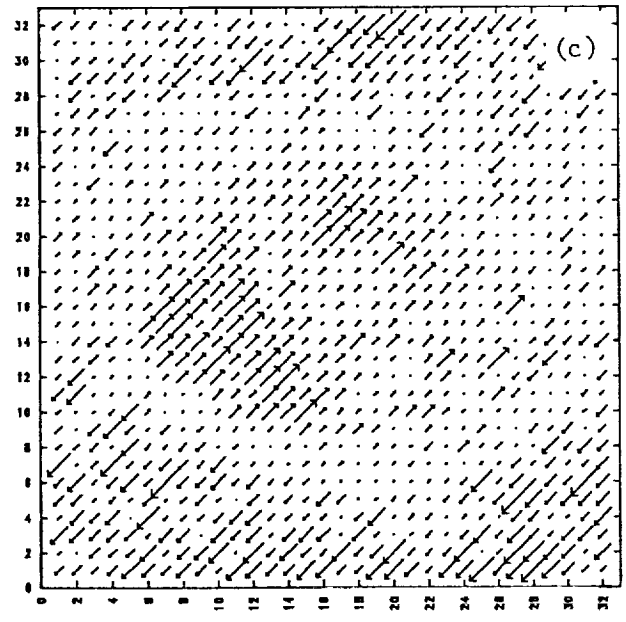


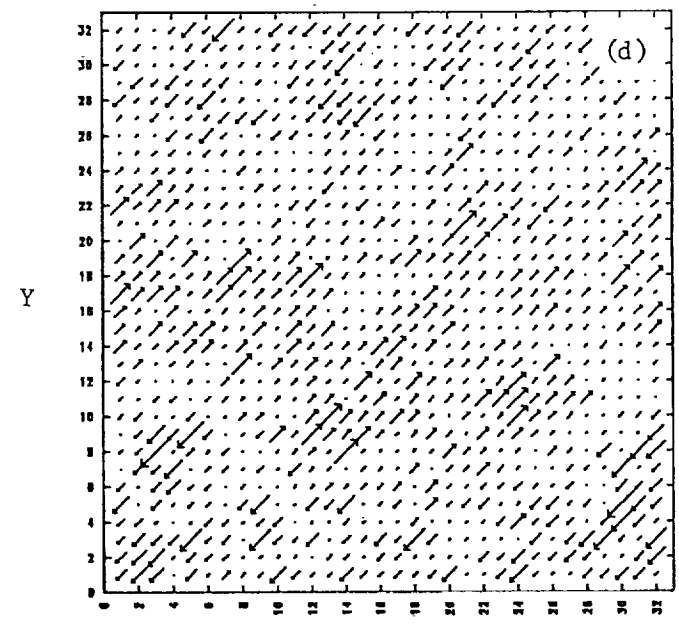


FIG. 11

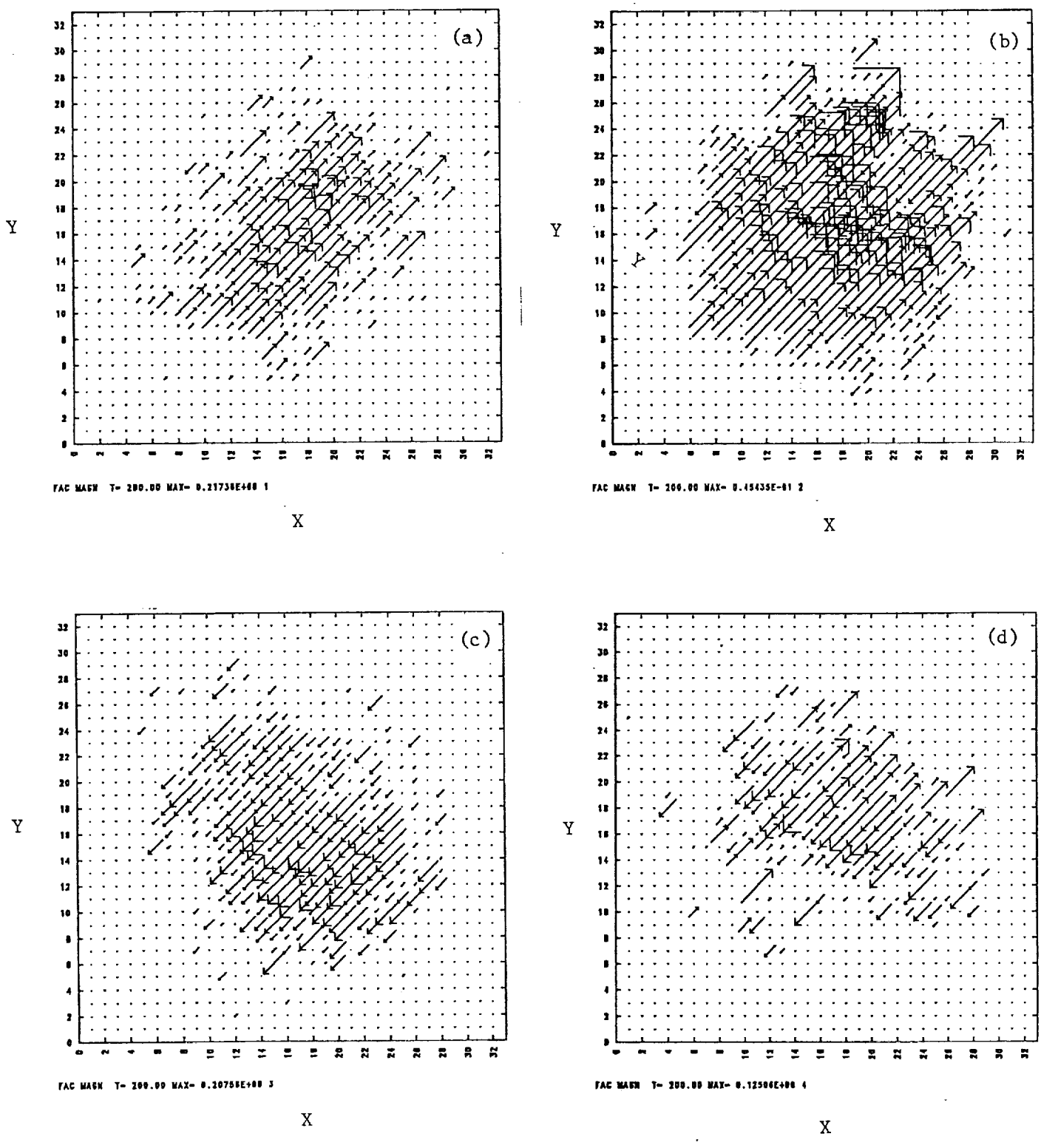


FIG. 12

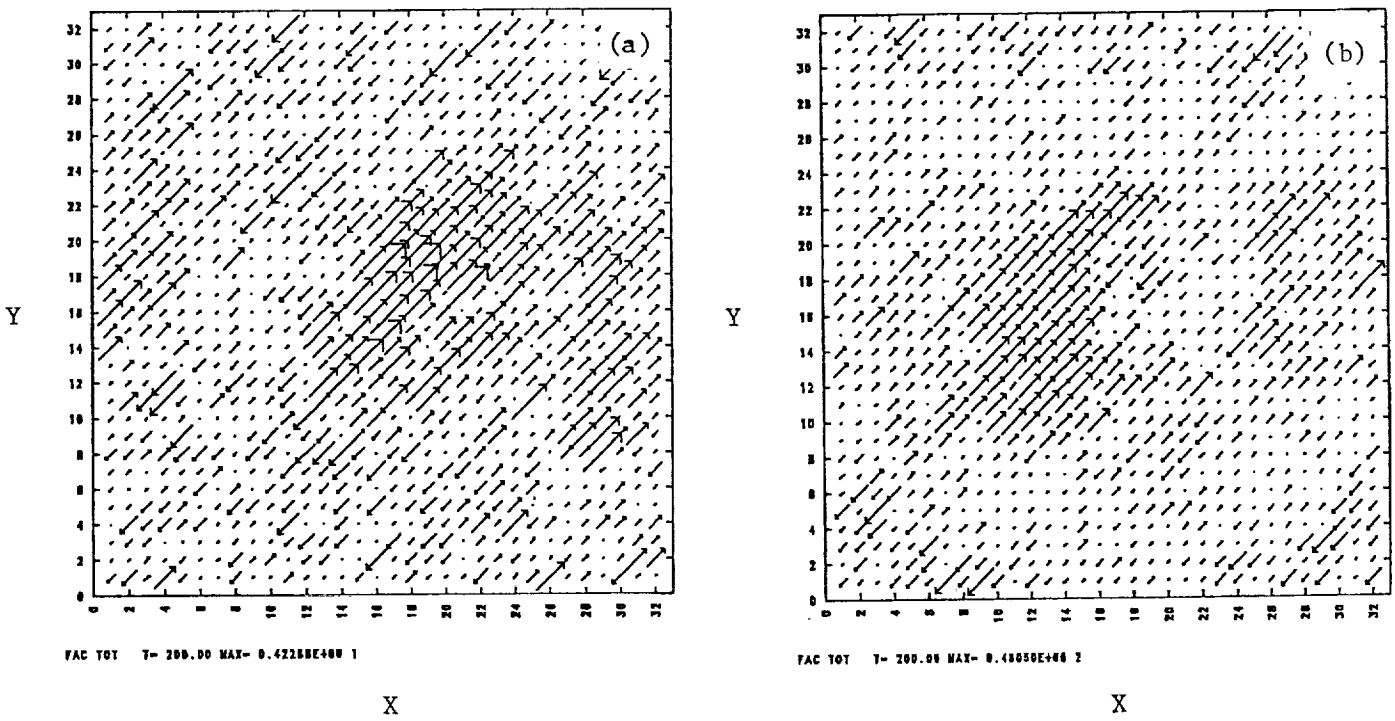


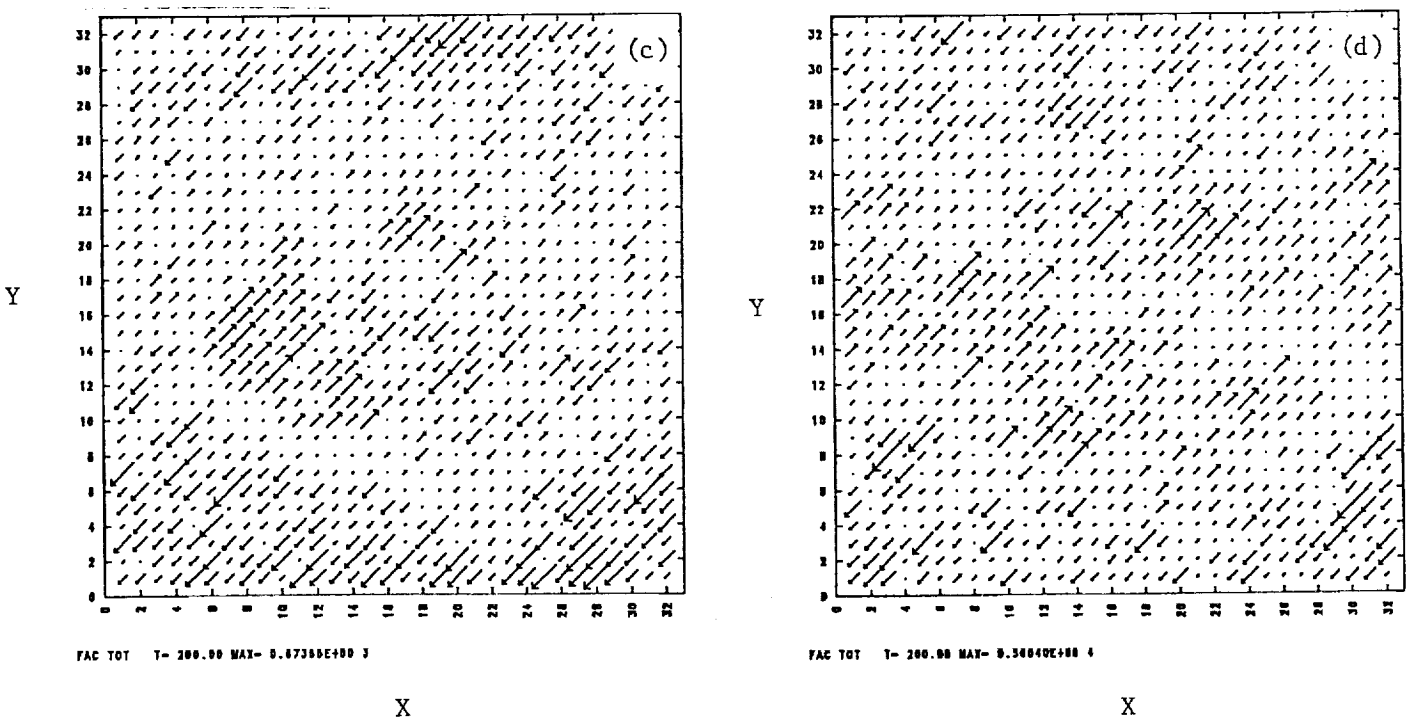


FIG. 13

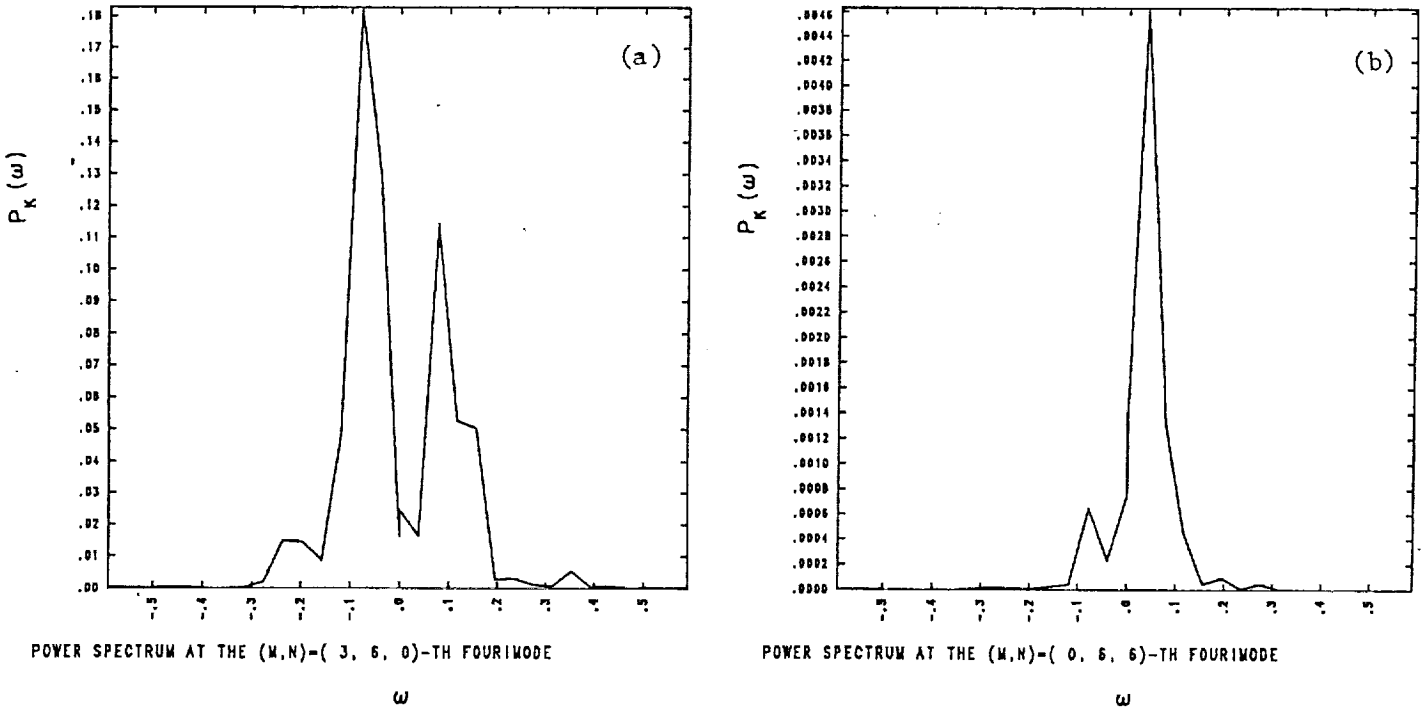
(a)
$P_K(\omega)$
POWER SPECTRUM AT THE (M,N)=( 3, 6, 0)-TH FOURIMODE
ω
(b)
$P_K(\omega)$
POWER SPECTRUM AT THE (M,N)=( 0, 6, 6)-TH FOURIMODE
ω

FIG. 14